Original Article

Study of Stress Distribution and Displacement of Various Craniofacial Structures Following Application of Transverse Orthopedic Forces—A Three-dimensional FEM Study

Alireza Jafari, MDS, M-Ortho[a]; K. Sadashiva Shetty, MDS[b]; Mohan Kumar, BE (Mech), ME (Design), MISTE, PhD[c]

Abstract: The purpose of this study was to analyze the stress distribution patterns within the craniofacial complex during rapid maxillary expansion. Therefore, a finite element model of a young human skull was generated using data from computerized tomographic scans of a dried skull. The model was then strained to a state of maxillary expansion simulating the clinical situation. The three-dimensional pattern of displacement and stress distribution was then analyzed. Maximum lateral displacement was 5.313 mm at the region of upper central incisors. The inferior parts of the pterygoid plates were also markedly displaced laterally. But there was minimum displacement of the pterygoid plates approximating the cranial base. Maximum forward displacement was 1.077 mm and was seen at the region of the anteroinferior border of the nasal septum. In the vertical plane, the midline structures experienced a downward displacement. Even the ANS and point A moved downward. The findings of this study provide some additional explanation of the concept of correlation between the areas of increased cellular activity and the areas of dissipation of heavy orthopedic forces. Therefore, the reason for the occurrence of sensation of pressure at various craniofacial regions, reported by the patients undergoing maxillary expansion could be correlated to areas of high concentration of stresses as seen in this study. Additionally, the expansive forces are not restricted to the intermaxillary suture alone but are also distributed to the sphenoid and zygomatic bones and other associated structures. (*Angle Orthod* 2003;73:12–20.)

Key Words: Rapid maxillary expansion (RME); Finite element model (FEM); Stress distribution; Displacement; Maxilla

INTRODUCTION

Rapid maxillary expansion (RME) is indicated in the treatment of maxillary deficiency. During RME, high forces are directed to the maxillary basal bone and perhaps to other adjacent skeletal bones. Such heavy RME forces can easily split the midpalatal suture in young individuals and force the two maxillary halves laterally.[1–8]

Widening has been reported to be associated with sensations of pressure at various craniofacial areas, especially in the areas of articulation of maxilla (for example, under the eyes and at the nasal area).[9] Similar histological studies on animals demonstrated a sign of increased cellular activity at various craniofacial sutures.[10–14] In relation to Wolff's law of bone transformation and stresses, this seems to point to the force concentration in these areas.

Where are the areas of maximum force concentration? How do these heavy forces get gradually dissipated? Moreover, is there the possibility of transmission of forces far enough to the base of the skull with possibility of distortion of sphenooccipital synchondrosis?[10]

It was difficult, if not impossible to answer the above questions by using conventional methods namely, strain gauge, photoelastic, or laser holographic techniques. But in recent years, finite element (FE) analysis has been introduced to orthodontics as a powerful research tool for solving various structural mechanical problems. It is recognized as a general procedure for mechanical approximation to all physical problems that can be modeled by deferential equation description.

FE analysis has been applied to the description of phys-

[a] Assistant Professor, Department of Orthodontics and Dentofacial Orthopedics, Bapuji Dental College, Davangere, India.
[b] Profesor and Head, Department of Orthodontics and Dentofacial Orthopedics, Bapuji Dental College, Davangere, India.
[c] Associate Professor, Department of Mechanical Engineering Bapuji Institute of Engineering and Technology, Davangere, India.
Corresponding author: Alireza Jafari, Assistant Professor, Department of Orthodontics and Dentofacial Orthopedics, Bapuji Dental College, Davangere-577 004 Karnataka, India.
(e-mail: alirezajafari@rediffmail.com)

Revised and Accepted: June 2002. Submitted: November 2001.

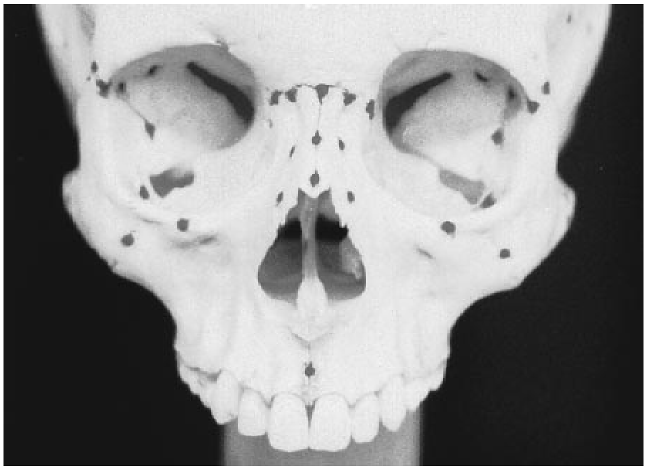

FIGURE 1. Dried young human skull used in this study.

ical form changes in biological structures, particularly in the form of growth and development and restorative dentistry. There are broadly two types of application in biomechanical studies. One is the analysis of stress and strain with a given force system applied to the teeth or the cranial complex. The other is the evaluation of the craniofacial growth with the given skeletal displacement observed during the growth changes.[15]

This study was planned to explore more in detail how heavy transverse orthopedic forces generated by RME get dissipated within the craniofacial complex. Therefore, the aim of this study was to evaluate the pattern of stress accumulation, dissipation, and displacement of various craniofacial structures after RME, using a three-dimensional FE study.

MATERIALS AND METHODS

In this study the analytical model was developed from a dry young human skull of a female with an approximate age of 12 years. The skull excluding the mandible was checked for the full complement of the permanent dentition and gross defects or discontinuity in the craniofacial anatomy. The anatomical structures such as sutures become indistinguishable with computerized tomographic (CT) scanning. Therefore, traces were placed in the form of barium sulfate pellets in 0.25-mm circular pits, which were made at three points along each of the craniofacial sutures (Figure 1). This was to transfer the precise location of the various sutures onto the finite element model (FEM).

CT scan images of the skull excluding the mandible were taken in the axial direction, parallel to the Frankfort horizontal plane. Sequential CT images were taken at 5-mm intervals to reproduce finer and detailed aspects of the geometry (Figure 2). This methodology of model creation was aimed at improving over the previous methodologies, where sections were taken at 10 mm intervals.[16]

The individual CT scan sections were traced on an acetate paper, taking care so as not to distort the anatomy of the region. This was enlarged to 200 times and traced onto the graph paper for digitization. Along the centerline of bone, of each CT image, geometric points were defined and assigned X, Y, and Z coordinates, which were fed into the preprocessor of the software for grid generation. The FE program used in this study was NISA-II Display-III and was run on a Pentium-III computer. The grids created were then joined to form lines (Figure 3). The geometric lines

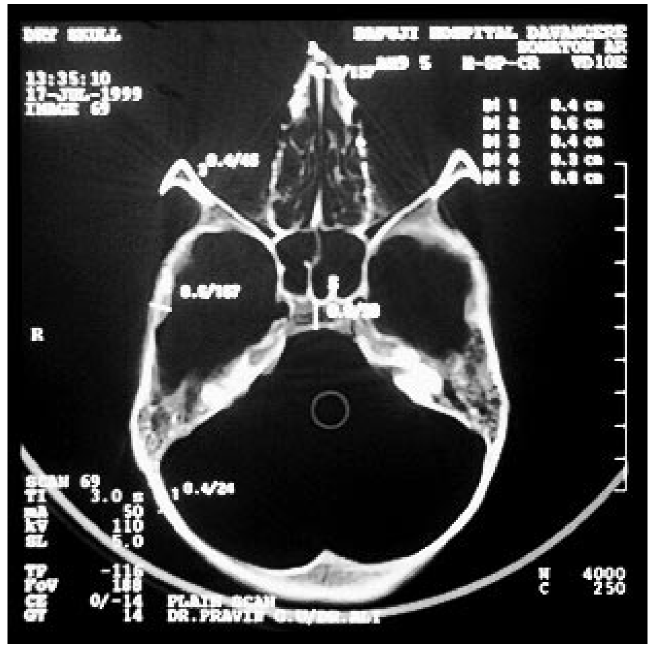

FIGURE 2. Scan image at the level of midorbital cavity.

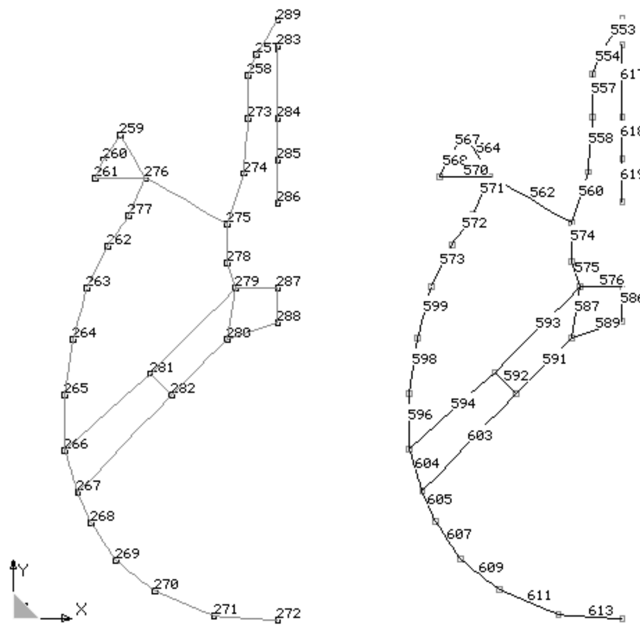

FIGURE 3. The digitized X,Y, and Z coordinates were fed into the computer to create grids and lines.

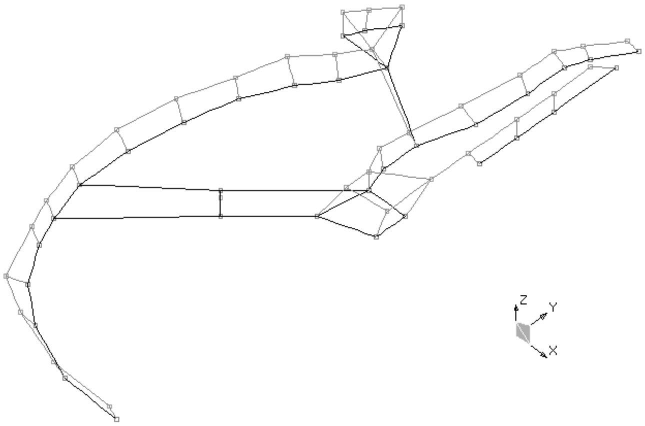

FIGURE 4. The geometric points between two neighboring layers were connected by straight lines forming flat triangular or quadrilateral surfaces between them.

passing through these points described the measured bone geometry as close as possible.

The next step was to generate geometric surfaces by joining lines together. Each layer created was stacked one above the other in the axial direction and joined by straight lines (Figure 4). Lines were joined to create patches. Only one half of the cranium with respect to the sagittal plane was modeled and analyzed. Analysis of the complete skull was not considered necessary because the analysis of one half of the cranium will produce the same results as that of complete skull.

The next step was to convert the geometric model into a FEM. The geometric entities created in the previous step were replaced with finite elements and nodes at this stage. The complete geometry is now defined as an assemblage of discrete pieces called elements and are connected together at a finite number of points called nodes. In this study a linear four nodal quadrilateral and triangular shell elements were used, which were able to take membranes into account, ie, in-plane deformation as well as bending deformations. The shell elements have six degrees of freedom (DOF) at each of their unstrained nodes: three translations (X, Y, and Z) and three rotations (around the X, Y, and Z axes). In the present study the model consisted of 44142 DOF, which gives a more consistent result as compared with previously published studies.[16–18] The total number of elements and nodes created was 6951 and 7357, respectively (Figure 5).

The mechanical properties of the compact and cancellous bones and teeth in the model were defined according to the experimental data in previous studies[16,17] as shown in Table 1. All the craniofacial sutures that were integrated in the

TABLE 1. Young's modulus and Poisson's ratio for various materials used in this study (Tanne et al)[16]

Material	Young's Modulus kg/mm^2	Poisson's Ratio
Tooth	2.0×10^3	0.3
Compact bone	1.37×10^3	0.3
Cancellous bone	7.9×10^2	0.3

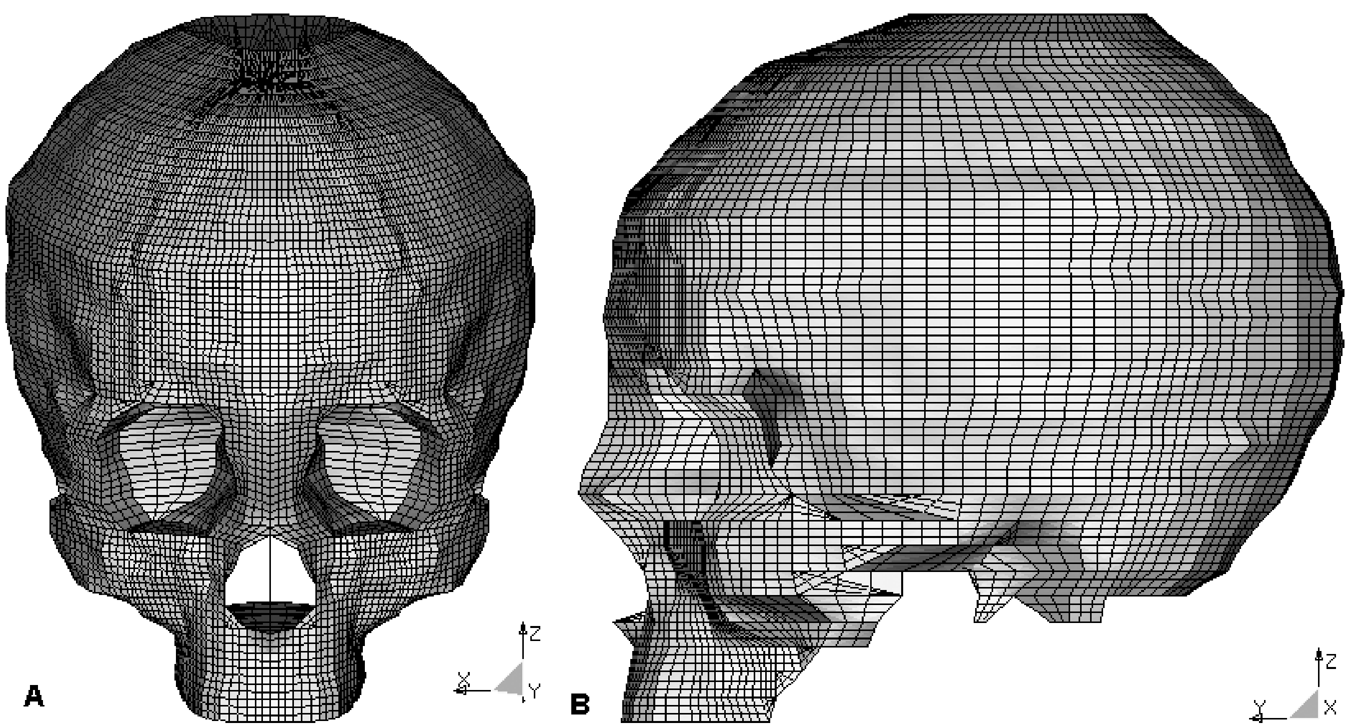

FIGURE 5. (A) Frontal and (B) lateral views of the final three-dimensional finite element model.

model were assumed to have the same mechanical properties as the surrounding bone material.[16–18]

Restrains were established at all other nodes of the cranium lying on the symmetrical plane, and appropriate boundary conditions were imposed. In addition, a zero-displacement and zero-rotation boundary condition was imposed on the nodes along the foramen magnum.

It is a well known fact that the midpalatal suture separates after initial application of heavy orthopedic forces.[1,3,8,10,13] Even though the midpalatal suture element was created in this study, the nodes of this suture that were placed on the symmetrical plane were left unconstrained. This was done to investigate the stress distribution and deformation of the craniofacial complex after splitting of the midpalatal suture.

Even though application of a known force is possible with FE modeling, but for the purpose of comparison with the previously published study,[18] a known transversal (X) displacement with a magnitude of 5 mm was applied on the maxillary premolars and first permanent molar crown. It was assumed that the two plates of transversal orthopedic appliance moved apart by a total distance of 10 mm.

The displacements, von Mises stresses, and shear stress in different planes were studied. The stress distribution patterns were analyzed; the results were tabulated and graphically represented. Because most of the stress was generated along the maxillary bone, a detailed analysis of this region was also carried out.

RESULTS

The biomechanical changes observed in this study were evaluated under the headings

- Displacement of different bones of craniofacial complex (Figure 6)
- Stress distribution among different bones and sutures (Figure 7).

Table 2 shows the three-dimensional pattern of displacements observed at 34 different anatomical structures located in the craniofacial complex.

Displacement in the transverse plane (X-displacement)

Maximum X-displacement (lateral displacement) was 5.313 mm at Node 12911, which corresponds to the incisal edge of the upper central incisor. Pyramidal displacement of maxilla away from the midline was evident from the frontal view. The base of the pyramid was located on the oral side and the apex faced the nasal bone. Viewed occlusally, the two halves of the maxillary dentoalveolar complex, basal maxilla, and lateral walls of the nasal cavity separated more widely, anteriorly. The width of the nasal cavity at the floor of the nose increased markedly, whereas the posterosuperior part of the nasal cavity had moved min-

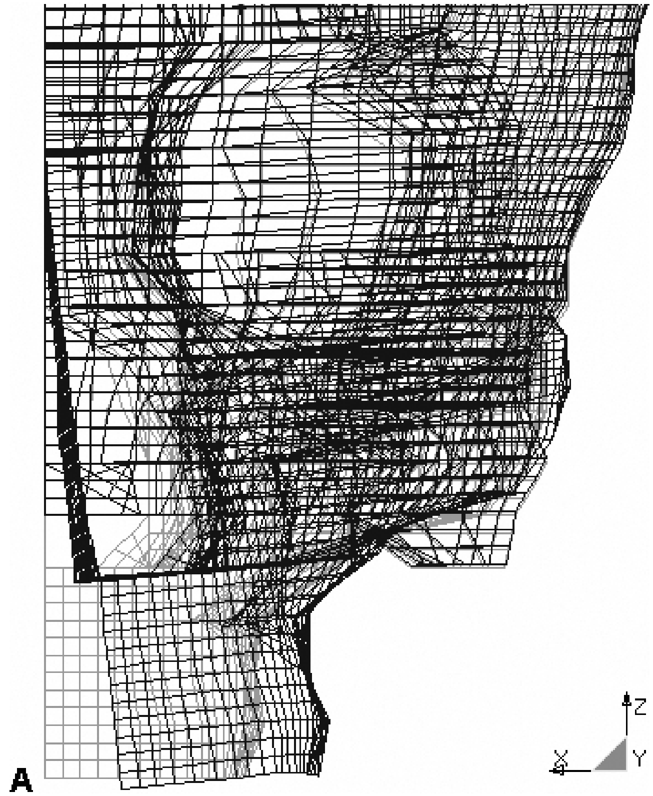

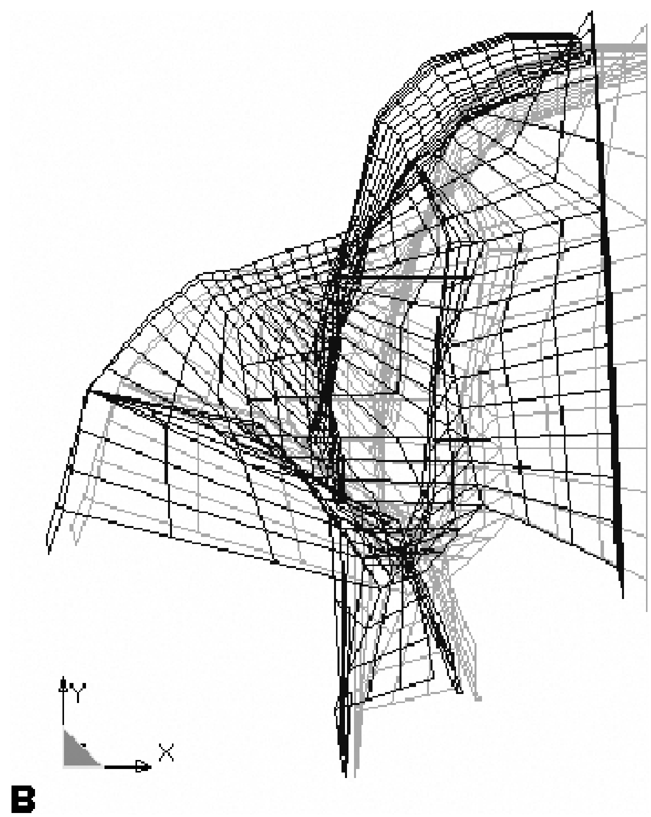

FIGURE 6. Pattern of deformation of the craniofacial complex with five mm of transverse expansion seen from (A) frontal view and (B) cranial view of the cut section of the maxilla just above the palatal vault.

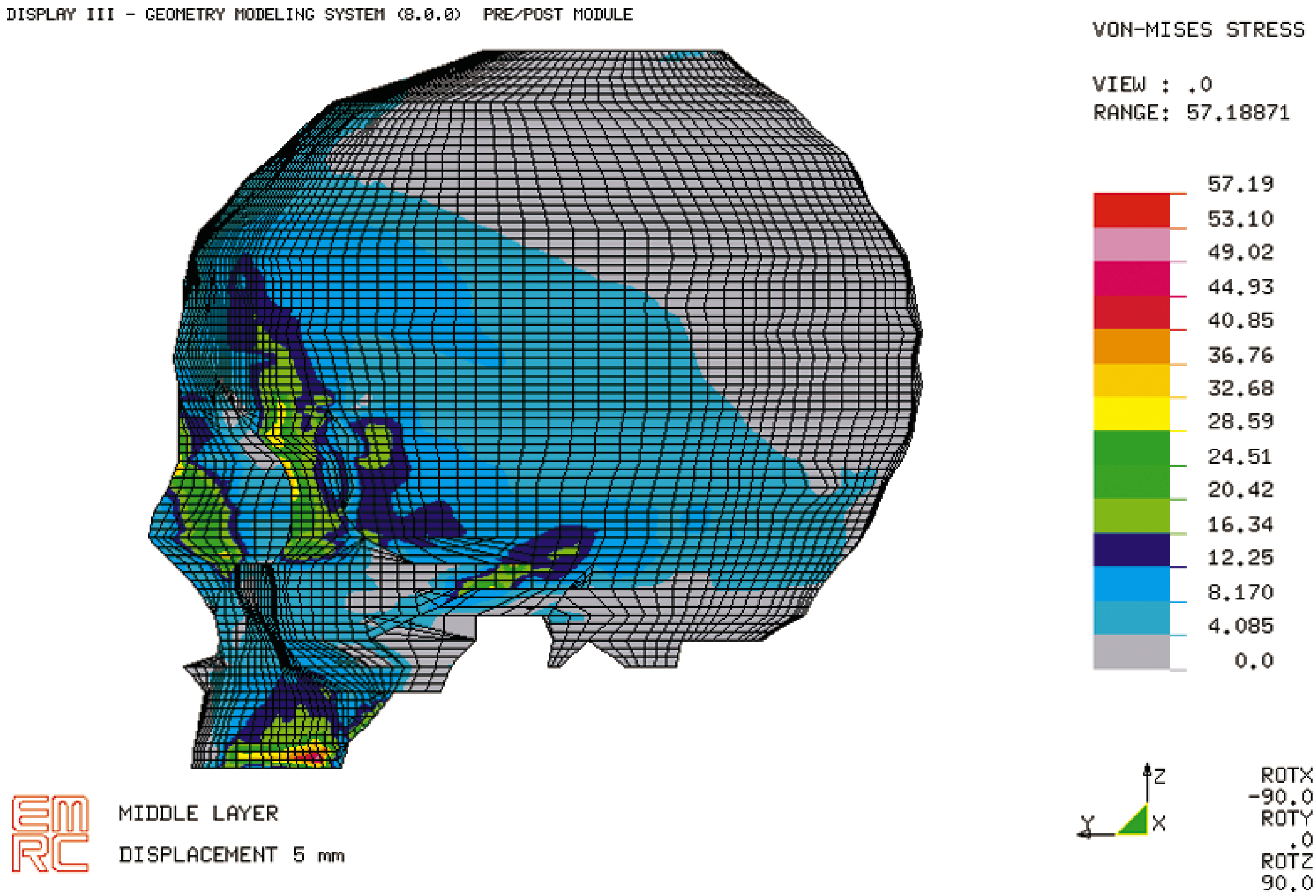

FIGURE 7. The pattern of computed Von-Mises stress distribution in the craniofacial complex with five mm of expansion.

imally in the lateral direction. No significant lateral displacement was observed at the temporal, parietal, frontal, sphenoid, and occipital bones. The inferior parts of the pterygoid plates were markedly displaced or bent laterally. But minimum displacement was observed in the region close to the cranial base, where the plates were more rigid.

Displacement in the anteroposterior plane (Y-displacement)

Maximum negative Y-displacement (backward displacement) was 1.159 mm at Node 2314, which corresponds to the posterior rim of the frontal process of the zygomatic bone, indicating that this portion of the craniofacial complex has moved posteriorly. Maximum positive Y-displacement (forward displacement) was 1.077 mm at Node 6022, which represents the anteroinferior border of the nasal septum. Maxillary bone, maxillary central incisors, and molars were slightly displaced forward. But the zygomatic bone showed a backward displacement.

Displacement in the vertical plane (Z-displacement)

Maximum negative Z-displacement (downward displacement) was 1.220 mm at Node 52, which represents the posterior most portion of the nasal septum; this indicates a downward displacement of structures medial to the area of force application. Maximum positive Z-displacement (upward displacement) was 1.758 mm at Node 241, which represents the body of the zygomatic bone. Considering both these points, it is evident that the nasomaxillary complex rotated in such a manner that the lateral structures had moved upward and midline structures downward. The anterior part of the maxillary bone (ANS and point A) and maxillary central incisors were displaced downward.

The magnitude and distribution of von Mises stresses produced at various sutures of the craniofacial complex by the activation of the RME device up to 5 mm on each side are shown in Table 3. Initial stress images of the three-dimensional model of the skull are shown below (Figure 7). The areas of stress are shown with the help of different colors. The pellets of colors representing the tensile and compressive stresses are shown on the right-hand side of the diagram.

Using the computer-generated color diagrams the following results were obtained. In the maxillary region, a compressive stress of 57.19 kg/mm^2 was observed over the region of the crown of the first permanent molar. The rest of the dentoalveolar regions from canine to molar also expe-

TABLE 2. Computational result of the transversal (X), sagittal (Y), and vertical (Z) displacement of the various skeletal structures of the craniofacial complex following 5 mm of transverse expansion

Region	Selected Nodes On	X, mm	Y, mm[a]	Z, mm[a]
Dentoalveolar	Incisal edge of 1	5.31	0.85	0.45
	Cusp tip of 3	5.09	0.71	0.33
	Cusp tip of 6	5.13	0.74	0.26
	Apical region of 1	4.34	0.85	−0.59
	Apical region of 3	3.94	0.50	0.26
	Apical region of 6	4.08	0.49	0.29
Maxilla	Point "a"	4.08	0.97	−0.84
	ANS	3.87	1.02	−0.86
	Tuberosity	3.65	0.42	0.22
	Zygomatic buttress	2.89	0.02	0.79
	Inferior orbital rim	1.85	−0.12	0.72
	Frontal process	0.97	0.09	−0.15
Palate	Anterior	3.22	1.03	−0.61
	Posterior	2.06	1.05	−1.02
Nasal cavity wall	Anteroinferior	3.25	0.52	0.00
	Anterosuperior	1.26	0.16	−0.02
	Posteroinferior	2.17	0.51	−0.26
	Posterosuperior	0.65	0.02	−0.02
Nasal bone	Body	0.23	−0.50	−0.59
Sphenoid bone	Body	0.00	0.00	0.00
	Medial pterygoid—inferior	1.86	−0.49	−0.37
	Medial pterygoid—superior	0.21	−0.06	0.15
	Lateral pterygoid—inferior	2.07	0.59	−0.44
	Lateral pterygoid—superior	0.44	0.08	0.13
	Greater wing	0.49	−0.32	0.66
Zygomatic bone	Body	0.21	−0.75	1.59
	Frontal process	2.07	−0.98	1.42
	Zygomatic arch—anterior	0.44	−0.93	1.67
	Zygomatic arch—posterior	0.04	−0.38	0.06
Frontal bone	Supraorbital	0.01	−0.02	0.10
	Forehead	0.01	−0.02	0.09
Temporal	Squamous	0.60	−0.25	0.59
Parietal	Tuberosity	0.16	−0.25	0.35
Occipital	Squamous	0.01	−0.05	0.05

[a] Positive value (+) indicates an anterior movement in a sagittal (Y) plane and an upward movement in the vertical (Z) plane. Negative value (−) indicates a posterior movement in a sagittal (Y) plane and a downward movement in the vertical (Z) plane.

rienced high initial stresses of 16.34–24.51 kg/mm^2. The zygomatic buttress and maxillary tuberosity showed areas of high stress. High stresses also were found around the frontal process of the maxilla, nasomaxillary suture, nasofrontal suture, frontomaxillary suture, and zygomaticomaxillary suture. The nasal bone, nasomaxillary suture, and nasofrontal suture experienced compressive forces of up to 32.68 kg/mm^2. Areas around the frontozygomatic suture and almost the whole length of the frontal process of the zygomatic bone were fields of high stress. The anterior rim

TABLE 3. Computational result of the Von–Mises stress distribution on the various sutures of the craniofacial complex following 5 mm of transverse expansion

Sutures[a]	von Mises Stress Values, kg/mm^2		
	Maximum	Minimum	Average
Internasal	55.4	7.22	19.18
Nasofrontal	32.7	8.13	15.82
Nasomaxillary	25.6	12.8	19.46
Frontomaxillary	9.38	8.11	8.67
Zygomaticomaxillary	8.95	2.85	5.71
Zygomaticofrontal	33.0	4.11	14.42
Zygomaticotemporal	9.27	1.99	5.24

[a] Selected groups of nodes were chosen on the model to represent each suture, based on the barium sulphate marker used on the dry skull.

of the frontal process of the zygomatic bone received 32.68 kg/mm^2 of forces. Similarly, the zygomatic arch and the area of the zygomaticotemporal suture had experienced high levels of stress. An interesting finding of this study was the presence of high stress all along the nasal septum, radiating upward to deeper anatomic structures such as the body of sphenoid bone. In the frontal, parietal, temporal, and occipital bones, RME produced stress levels ranging from 0.0 to 4.085 kg/mm^2.

A comparison was made between the computational results of this study and a similar previously published study;[18] both the studies were carried out independent of each other. A comparison of displacement of various craniofacial skeletal units of the two studies has been summarized in Table 4 and accompanying graphs. However, as stress distribution at various craniofacial sutures was not tabulated in the previous study,[18] we did not establish any comparison of von Mises stress distributions.

Note that any variation in the values between the two studies could be attributed to the sample used for the generation of FEM or the model generated on the computer (or both) or selection of the nodes and elements on the FEM (or both).

We presume the selection of the nodes and elements on the FEM is the single most important element in showing variance; however the overall results are comparable except for a few differences, which are mentioned in the discussion.

DISCUSSION

The three-dimensional FEM used in the present study provides the freedom to simulate orthodontic force systems applied clinically and allows analysis of the response of the craniofacial skeleton to the orthodontic loads in three-dimensional space.

The FE analysis has the following advantages: it is a noninvasive technique; the actual amount of stress experienced at any given point can be theoretically measured; the tooth, alveolar bone, periodontal ligament, and craniofacial

TABLE 4. Comparison of the computational result of the transversal (X), sagittal (Y), and vertical (Z) displacement of the various skeletal structures of the craniofacial complex

Region	Selected Nodes On	X[a], mm	X, mm	Y[a], mm[b]	Y, mm[b]	Z[a], mm[b]	Z, mm[b]
Dentoalveolar	Incisal edge of 1	5.00	5.31	1.40	0.85	−1.40	−0.45
	Cusp tip of 6	5.00	5.13	1.40	0.74	−0.80	0.26
	Apical region of 1	4.99	4.34	2.10	0.85	−1.20	−0.59
	Apical region of 3	4.99	3.94	2.10	0.50	−1.10	0.26
	Apical region of 6	4.91	4.08	2.00	0.49	−0.40	0.29
Maxilla	Anterior part of plate	4.90	3.22	2.10	1.03	−1.10	−0.61
	Posterior part of plate	4.80	2.06	2.10	1.05	−0.20	−1.02
Sphenoid bone	Inferior part lateral pterygoid plates	4.90	2.07	1.80	0.59	−0.04	−0.44
	Superior part lateral pterygoid plates	1.40	0.44	1.60	0.08	−0.70	0.13
Zygomatic bone	Frontal process	3.90	2.07	1.60	−0.98	−0.40	1.42
	Anterior zygomatic arch	3.30	0.44	0.70	−0.93	0.40	1.67
	Posterior zygomatic arch	0.60	0.04	−0.04	−0.38	0.20	0.06
Nasal cavity	Anteroinferior wall	4.80	3.25	2.10	0.52	−1.10	0.00
	Anterosuperior wall	4.80	1.26	2.10	0.16	−0.02	−0.02
	Posterosuperior wall	−0.30	0.65	0.20	0.02	−1.10	−0.02
Nasal bone	Body	0.30	0.23	−1.20	−0.50	−1.10	−0.59
Frontal bone	Supraorbital	0.03	0.01	−0.20	−0.02	−0.50	0.10
Parietal	Tuberosity	0.00	0.16	−0.05	−0.25	−0.02	0.35
Temporal	Squamous	0.10	0.60	0.08	−0.25	0.40	0.59
Occipital	Squamous	0.002	0.01	−0.02	−0.05	−0.02	0.05

[a] Values taken from Iseri et al.[18]

[b] Positive value (+) indicates an anterior movement in a sagittal (Y) plane and an upward movement in the vertical (Z) plane. Negative value (−) indicates a posterior movement in a sagittal (Y) plane and a downward movement in the vertical (Z) plane.

bones can be simulated and the material properties of these structures can be assigned to the nearest one that possibly can simulate the oral environment in vitro; the displacement of the tooth can be visualized graphically; the point of application, magnitude, and direction of a force may easily be varied to simulate the clinical situation; reproducibility does not affect the physical properties of the involved material; and the study can be repeated as many times as the operator wishes.[15]

FEM is a powerful contemporary research tool, and plenty of literature is available on the study of stress distribution and deformation of nonliving as well as natural and restored craniofacial structures affected by three-dimensional stress fields, which are difficult to assess otherwise.[15–18] But experimental or clinical confirmation of the theoretical prediction should be the goal in any simulation study. In this FE analysis, direct validation of the theoretical results was not possible, therefore the results of the present study were compared with the results of the previously published human studies[3,5,7,8,19,20] and were found to be in conformity.

In previous studies on human[8,21] or animal[3,10,13] skulls, it was possible only to determine the response of surrounding bones to high-level forces, and the experiment could not be repeated. The experimental method employed in this study permitted the visualization of bone reactions, even with the lowest loading degree. One should be aware that the structural and spatial relationships of various craniofacial components vary among individuals. It is important to realize that these factors may contribute to varied responses of the craniofacial components on loading. Thus, the results of this study are valid only for a single specific human skull.

The wedge shape opening of the midline structure in this study was evident both in the vertical and anteroposterior plane. The results of the present study support those of the previous studies, which reported that the separations were pyramidal in shape, with the base of the pyramid located at the oral side of the bone and the center of rotation located near the frontonasal suture.[1,2,3,6,8,18]

Previous studies[3,8,18] have shown that in the frontal plane, the fulcrum of the rotation for each of the maxillae was approximately at the frontomaxillary suture. Using implants,[5] the maxillae were found to tip anywhere between −1 to +8 degrees relative to each other. Thus the findings of the previous studies regarding the transverse rotations of the nasomaxillary complex with RME are confirmed by the computational results of the present study.

Wertz[8] and Isaacson[22,23] suggest that the main resistance to midpalatal suture opening is probably not in the suture itself but in the surrounding structures of the sphenoid and zygomatic bones. Chaconas and Caputo[24] also mentioned a limiting factor for maxillary expansion, which may depend on the fusion or lack of fusion between the maxilla and pterygoid plates of the sphenoid bone. Melsen and Melsen[25] have shown that the heavy interdigitation of the osseous surfaces between the palatine bone and the maxilla and the pterygoid process of sphenoid bone makes disarticulation difficult in late juvenile and early adolescence periods. Timms[7] concluded that RME will separate the maxilla and palatine bones but would splay the pterygoid processes of the sphenoid bone outward because they are not bilaterally paired bones.

Similarly, comparatively less or no displacement of the pterygoid plates was seen in this study, and transmission of the expansion forces to the other parts of the sphenoid bone are suggestive of their role as a constraint on the transverse forces. Further indications of the deep anatomic effects of the transverse orthopedic forces were observed by the stress in the areas of the zygomatic processes, namely the zygomaticomaxillary and zygomaticotemporal sutures. The deep anatomical effects of these orthopedic appliances was also observed by the high stress levels in the areas of the maxillary bone, in the maxillary molar area, zygomatic process, external walls of the orbit, frontozygomatic suture, and frontal process of maxilla.

It has been reported previously that some of the patients subjected to RME feel pressure in the vault of the palate, in the region of the alveolar process, in the frontonasal region, under the eyes, and generally throughout the face.[9,24] Interestingly enough, these anatomical landmarks coincide with the area of high-stress distribution in the present FEM study.

Hass[3] and others[2,6,8,10,18,26] found the maxilla to be more frequently displaced downward and forward. The final position of the maxilla, after completion of expansion is unpredictable, and it has been reported to return, partially or completely, to its original position. Wertz[8] believed that the disjunction of the maxillopalatine complex from pterygoid process could provide a possible answer to few rare instances in which point A and the entire maxilla were moved forward by a significant amount. But Gardner and Kronman[10] believed the fact that the maxilla moving forward and downward during the expansion procedure was correlated with the opening of the sphenooccipital synchondrosis.

In this study, however, point A and ANS moved forward by 1.074 mm. This is in agreement with the above studies. But the opening of sphenooccipital synchondrosis could not be seen as a factor and, therefore, the restraining effect of the pterygoid plates of the sphenoid bone and the buttressing effect of the zygomatic bone could be the possible explanation for forward movement of the nasomaxillary complex.

The literature published on the vertical skeletal displacement of the upper jaw after RME agrees that the maxilla descends either parallel or rotates anteriorly or posteriorly.[3,4,8,20,27] But all authors do not agree on this point.[2] The analytical result of the present study showed that the palate moved slightly downward, more in the posterior than anterior, displaying a forward rotation in the palatal plane.

How far from the dentoalveolar region do the expansion forces affect the skeletal sutures? A number of authors reported that these forces can affect the other bones surrounding the maxillary complex.[6,8,10,18] In this study, however, those bones, which did not have a direct sutural articulation with the maxilla and palatine bones, showed comparatively little or no displacement at all. But many investigators have pointed out that RME is not only limited to the palatal region but also causes dramatic changes in the craniofacial structures. Gardner and Kronman[10] in a study of RME on rhesus monkeys found that the lambdoid, parietal, and midsagittal sutures of the vault of the cranium showed evidence of distortion, and in one animal a split of 1.5 mm was reported.

An increase in nasal width has been demonstrated as a response to RME.[3,4,6,8,18] The numerical results of the present study demonstrate that the width of the nasal cavity at the floor of the nose increased markedly compared with the superior part. This result is similar when compared with the Pavlin and Vukicevik study.[21] Therefore a combination of increase in nasal width, lowering of palatal plane, and probably straightening of the nasal septum after RME can help the patients with nasal stenosis. Wertz[28] and Hershey et al[29] have recorded reduction in nasal airway resistance after rapid maxillary expansion.

The results of the present study using the three-dimensional FEM of a human skull provided some additional explanation about the bony tissue mechanical reactions, which are the first steps in the compound process of tissue response to jaw expansion. Acquaintance with these initial mechanical reactions helps the orthodontist to understand better the final therapeutic effects and the way the orthodontic appliance actually acts on the basal bones and sutures of the craniofacial system.

CONCLUSIONS

The results of the present study using the three-dimensional FEM of a human skull indicted that the transverse orthopedic forces not only produced an expansive force at the intermaxillary suture but also high forces on various structures on the craniofacial complex, particularly the sphenoid and zygomatic bones.

The confining effect of the pterygoid plates of the sphenoid minimizes dramatically the ability of the palatine bones to separate at the midsagittal plane. Further posteriorly, the pterygoid plates can bend only to a limited extent because pressure is applied to them, and their resistance to bending increases significantly in the parts closer to the cranial base where the plates are much more rigid. Therefore, the clinician should realize that with activation of the RME appliance he/she is producing not only an expansion force at the intermaxillary suture but also forces on other structures within the craniofacial complex that may or may not be beneficial for the patient.

It should be noted that during surgically assisted RME, release of the pterygoid plates is necessary because, unlike the maxilla, which is the paired bone, the sphenoid is a single bone with both pterygoid processes attached. Therefore, the pterygoid processes must be separated from the maxilla to allow posterior maxillary expansion.

Because of their relative rigidity, skeletal tissues offer immediate resistance to expansion force. But another equally important factor is the soft tissue complex that invests these skeletal structures. The muscles of mastication, the facial muscles, and the investing fascia are relatively elastic and can be stretched as the expansion forces are applied. But the ability of the stretched muscles, ligaments, and fascia to permanently adapt to the new environment is a matter that deserves further investigation.

ACKNOWLEDGMENTS

The authors would like to thank Drs. Benoy Mathew, A. V. Arun, Abdul Hakeem, Govardhan Rao, Krishnakant Reddy, T. Ramanjulu, K. Divakar, K. Vani, Chetana Chandra, Sunil Sunny, Ashutosh Shetty and faculty members and students of the Department of Orthodontics and Dentofacial Orthopedics, Bapuji Dental College, Davangere, India.

REFERENCES

1. Cleall JF, Bayne D, Posen J, Subtelny JD. Expansion of the midpalatal suture in the monkey. *Angle Orthod.* 1965;35:23–35.
2. Davis WM, Kronman JH. Anatomical changes induced by splitting of the midpalatal suture. *Angle Orthod.* 1969;39:126–132.
3. Hass AJ. Rapid expansion of the maxillary dental arch and nasal cavity by opening the midpalatal suture. *Angle Orthod.* 1961;31:73–90.
4. Hass AJ. The treatment of maxillary deficiency by opening the midpalatal suture. *Angle Orthod.* 1965;35:200–217.
5. Hicks EP. Slow maxillary expansion a clinical study of the skeletal versus dental response to low-magnitude force. *Am J Orthod.* 1978;73:121–141.
6. Memikoglu TUT, Iseri H. Effects of a bonded rapid maxillary expansion appliance during orthodontic treatment. *Angle Orthod.* 1999;69:251–256.
7. Timms DJ. A study of basal movement with rapid maxillary expansion. *Am J Orthod.* 1980;77:500–507.
8. Wertz RA. Skeletal and dental changes accompanying rapid midpalatal suture opening. *Am J Orthod.* 1970;58:41–66.
9. Zimring JF, Isaacson RJ. Forces produced by rapid maxillary expansion. Part II. Forces present during retention. *Angle Orthod.* 1965;35:178–186.
10. Gardner GE, Kronman JH. Cranioskeletal displacement caused by rapid palatal expansion in the Rhesus monkey. *Am J Orothod.* 1971;59:146–155.
11. Starbach H, Bayne D, Cleall J, Subtelny JD. Facioskeletal and dental changes resulting from rapid maxillary expansion. *Angle Orthod.* 1966;36:152–164.
12. Starnbach HK, Cleall JF. The effects of spliting the midpalatal suture on the surrounding structures. *Am J Orthod.* 1964;50:923–924.
13. Storey E. Tissue response to the movement of bones. *Am J Orthod.* 1973;64:229–247.
14. Ten Cate AR, Freeman E, Dickinson JB. Sutural Development: structure and its response to rapid expansion. *Am J Orthod.* 1977;71:622–636.
15. Korioth TWP, Versluis A. Modeling the mechanical behaviour of the jaws and their related structures by finite element (FE) analysis. *Crit Rev Oral Biol Med.* 1997;8:90–104.
16. Tanne K, Hiraga J, Kakiuchi K, Yamagata Y, Sakuda M. Biomechanical effect of anteriorly directed extraoral forces on the craniofacial complex: a study using the finite element method. *Am J Orthod Dentofac Orthop.* 1989;95:200–207.
17. Hiraga MJ, Tanne K, Nakamura S. Finite element analysis for stresses in the craniofacial sutures produced by maxillary protraction forces applied at the upper canines. *Br J Orthod.* 1994;21:343–348.
18. Iseri H, Tekkaya AE, Oztan O, Bilgic S. Biomechanical effect of rapid maxillary expansion on the craniofacial skeleton, studied by the finite element method. *Eur J Orthod.* 1998;20:347–356.
19. Isaacson RJ, Murphy TD. Some effect of rapid maxillary expansion in cleft lip and palate patients. *Angle Orthod.* 1964;34:143–154.
20. Wertz R, Dreskin M. Midpalatal suture opening—a normative study. *Am J Orthod.* 1977;71:367–381.
21. Pavlin D, Vukicevic D. Mechanical reactions of facial skeleton to maxillary expansion determined by laser holography. *Am. J. Orthod.* 1984;85:498–507.
22. Isaacson RJ, Ingram AH. Forces produced by rapid maxillary expansion. Part II. Forces present during treatment. *Angle Orthod.* 1964;34:261–270.
23. Isaacson RJ, Wood JL, Ingram AH. Forces produced by rapid maxillary expansion. Part I. Design of the force measuring system. *Angle Orthod.* 1964;34:256–260.
24. Chaconas SJ, Caputo AA. Observation of orthopedic force distribution produced by maxillary orthodontic appliances. *Am J Orthod.* 1982;82:492–501.
25. Melson B, Melsen Flemming. The postnatal development of the palatomaxillary region studies on human autopsy material. *Am J Orthod.* 1982;82:329–342.
26. Cotton LA. Slow maxillary expansion: skeletal versus dental response to low magnitude force in Macaca mulatta. *Am J Orthod.* 1978;73:1–23.
27. Fried KH. Palate—tongue relatively. *Angle Orthod.* 1971;61:308–323.
28. Wertz EA. Changes in nasal airflow incident to rapid maxillary expansion. *Angle Orthod.* 1968;38:1–11.
29. Hershey HG, Stewart BL, Warren DW. Changes in nasal airway resistance associated with rapid maxillary expansion. *Am J Orthod.* 1976;69:274–284.